https://doi.org/10.5194/nhess-2021-284
Preprint. Discussion started: 26 January 2022

Natural Hazards and Earth System Sciences
Discussions

Modelling the compound flood hydrodynamics under mesh convergence and future storm surge events in Brisbane River Estuary, Australia

Usman Khalil [1,*], Shuqing Yang [1], Muttucumaru Sivakumar [1], Keith Enever [1], Muhammad Zain Bin Riaz [1], Mariam Sajid [2]

[1] School of Civil, Mining and Environmental Engineering, University of Wollongong, NSW 2522, Australia

[2] School of Architecture and Design, University of Engineering and Technology Lahore, 54890, Lahore Pakistan

* Corresponding Author: Usman Khalil (uk998@uowmail.edu.au)

https://doi.org/10.5194/nhess-2021-284
Preprint. Discussion started: 26 January 2022

Natural Hazards and Earth System Sciences
Discussions

Abstract: Floods are the most common and destructive disasters around the globe, which becomes more challenging in coastal areas due to higher population density and catchment area relative to floods in an inland area. For effective coastal flood management to reduce flood adverse impacts it is necessary to investigate the flooding processes and their joint interaction in a coastal area. This paper selected the Brisbane River Estuary, Australia as an example and the MIKE 21 model is applied to investigate the effects of mesh resolution on the flood discharge and to explore compound flooding by computing variances in coastal flood assessments resulting from a separation of tidal and riverine processes. The statistical results showed that the Nash-Sutcliffe coefficient, E of water level are varied from 0.84 to 0.95 and the model simulated the 2011 flood extent results agreed with 90% accuracy with the observed flood extent. Five mesh resolutions cases were analyzed and the result found that the finer mesh resolution Case 5 was more appropriate for calculating the peak discharge with 2.7% with estimated discharge. Compound flood event simulation results emphasized that not considering the interaction of various flooding drivers caused 0.62 m and 0.12 m reduction in the flood levels at Jindalee and Brisbane city gauges, and uncertainties in flood extent. Simulated results of flood at Brisbane city gauge, showed that 2011 and 2013 floods with storm surge scenario 4 demonstrate, the increase in flood level to be 12% and 34% respectively. The results recommend flooding assessment by using mesh convergence with joint probability of compound flood under future storm surge for planning and management of coastal projects.

Keywords: Compound flood, hydrodynamic model, MIKE 21, Mesh size, storm surge

1 Introduction

Flooding is a prevalent and most destructive catastrophe worldwide, which poses a severe threat to lives and properties (Geravand, Hosseini, & Ataie-Ashtiani, 2020; Khalil & Khan, 2017; X. Liu & Lim, 2017). Coastal flooding is likely to increase in the future (Sadler, Goodall, Behl, Bowes, &

https://doi.org/10.5194/nhess-2021-284
Preprint. Discussion started: 26 January 2022

Morsy, 2020) due to sea-level rise, increased storm surge, land subsidence and urbanization (Pachauri et al., 2014; Van Coppenolle & Temmerman, 2019; Vitousek et al., 2017). Flooding has caused a global economic loss of $US 70.1 billion between 2000-2015 (Geravand et al., 2020), affecting 2.3 billion people (Hallegatte, Green, Nicholls, & Corfee-Morlot, 2013). It is anticipated that global flood losses will hit USD one trillion per year in 2050 (Lee & Kim, 2018; McCallum et al., 2016; Sulis, Frongia, Liberatore, Zucca, & Sechi, 2018; Tsoukala et al., 2016; UNISDR, 2015). For instance, in South East Queensland (SEQ), Australia the 2011 flood affected more than 2.5 million people and around 29,000 homes in the Brisbane River Valley (Barton, Wallace, Syme, Wong, & Onta, 2015; Syme, Wallace, Rodgers, Jensen, & Barton, 2019), the flooding led to 35 deaths and AUD2.55 billion economic loss (van den Honert & McAneney, 2011). In coastal catchments, floods can be produced by runoff generated by a significant rainfall event (Neumann et al., 2014) and a raised ocean level produced by a storm surge, or a combination of both. A storm surge is the rise of water level above the normal sea level along a coast due to reduced atmospheric pressure and/or strong coastal winds (Karim & Mimura, 2008). The storm surge influences may further increase when they coincide with riverine flooding (Zheng, Westra, Leonard, & Sisson, 2014) and the resulting combination is known as compound flood events (Leonard et al., 2014; Wu, Westra, & Leonard, 2020). Initially, the two involved flooding drivers involved were managed individually in coastal flood management (Torres et al., 2015). However, studies show that storm surge and extreme rainfall processes are statistically dependent, and thus their joint interface needs to be considered (Hawkes & Svensson, 2006; Svensson & Jones, 2004; Zheng, Westra, & Sisson, 2013). For an effective coastal flood inundation assessment, multiple measures, such as flood assessment models using good resolution digital elevation data (DEM) and considering a compound flood event with future storm surges are required to be implemented to reduce flood adverse impacts. In the past various researchers have given substantial efforts to simulate flood inundation in the

https://doi.org/10.5194/nhess-2021-284
Preprint. Discussion started: 26 January 2022

coastal floodplain with different numerical modelling approaches (Chen, Evans, Djordjević, & Savić, 2012; Son, Kim, & Han, 2016). Modelling approaches considered were (1) empirical approaches such as measurements (O'Connor & Costa, 2004) and remote sensing (Smith, 1997), (2) hydrodynamic models; (3) conceptual models for big floodplain areas (Teng et al., 2017) and probabilistic flood risk assessment (Apel, Thieken, Merz, Blöschl, & Sciences, 2004). While, the hydrodynamic models and in particular 2D models were the most used tools to simulate flood hydrodynamics, flood extent, flood forecasting and scenario analysis (Teng et al., 2017) because they simulate features in x and y directions at every mesh point interval, and take fewer computation times as compared to 3D model (X. Liu & Lim, 2017; Shrestha et al., 2020; Yu, 2017). Further, flood hydrodynamic modelling has significantly improved with the advanced approaches including digital elevation models (DEMs). Flood modelling simulation accuracy mainly depends on the suitable discretization of the geometric domain and grid resolution of the DEM (Geravand et al., 2020). Literature review revealed that existing studies have used various resolution DEM data with and without considering the compound flood and future storm surge events effects (Kumbier, Cabral Carvalho, Vafeidis, & Woodroffe, 2018). For instance, Karim and Mimura (2008) studied the influences of sea-level rise (SLR) on storm surge flooding in Western Bangladesh and hydrodynamic model simulation showed that for a storm surge under 0.3m SLR, the flooded area would enlarge by 15.3% of the current flooded area. Similarly, studies showed that higher resolution DEMs represents more exact terrain features which leads to more precise floodplain assessment and coarser-resolution DEMs over-predicted the extents of flood and caused substantial precision loss (Shrestha et al., 2020). However, there is no systematic framework for considering all the relevant flooding modelling parameters for effective flood assessment.

The recent flooding in summer 2021 has caused widespread damages across 20 countries (i.e. the USA to Italy, from China to India etc.) with 920 deaths (Copernicus, 2021). Further, climate change

https://doi.org/10.5194/nhess-2021-284
Preprint. Discussion started: 26 January 2022

Natural Hazards and Earth System Sciences
Open Access
Discussions

impacts assessments in IPCC recent report (IPCC, 2021) have urged us to consider and model future impacts and take remedial measures to reduce their impacts. Flooding events specify the need for a sustainable modelling approach to simulate the flood extent and propose measures to alleviate future flooding. To access the flood hydrodynamics, the Brisbane River Estuary (BRE) Australia were studied, which has been exposed to several flooding events over the past century, while, it has experienced two destructive flooding events in the year 2011 and 2013 when a storm surge coincided with extreme riverine discharge in the BRE (Queensland Floods Commission Inquiry Report, 2011). Earlier studies have utilized the 2D hydrodynamic model for Brisbane river flood modelling (X. Liu & Lim, 2017; Yu, 2017). However, the combined effect of riverine and tidal flooding was not considered, with the future effect of storm surge (Wu et al., 2020). For flood assessment and inundation mapping both temporal and spatial (flood depth and inundation extent) knowledge is required and can be applied in the flood risk analysis (X. Liu & Lim, 2017; Mani, Chatterjee, & Kumar, 2014). However, existing studies on the Brisbane River have used coarser-resolution geometric data, with 66.9% accuracy of flood modelling results, which leads to uncertainty and is less precise for coastal management. Other studies used hydrological and hydraulic models combination for BRE flood extent assessment, however, these models require extensive input data and further, it is restricted to government use and have limited access for research studies (Barton, Syme, Ryan, Rodgers, & Jensen, 2017). The complexity of the Brisbane river area for flood forecast by analyzing the compound flooding risks and considering future storm surge scenarios is still a significant and challenging study (Pellikka, Leijala, Johansson, Leinonen, & Kahma, 2018), which lead to the development of the hydrodynamic model for BRE for flood inundation.

This study examines and analyses BRE hydrodynamics by using MIKE 21 hydrodynamic model to investigate the flood extent with various mesh resolutions. Further, to understand the interaction of

https://doi.org/10.5194/nhess-2021-284
Preprint. Discussion started: 26 January 2022

storm-tide and fluvial flooding mechanisms, we investigate a compound flood event in a BRE to quantify how changing boundary set-ups at the entrance in Moreton Bay affect modelled water levels and flood extent of the study area. In this paper, we address several of the issues outlined above; the objectives of this study are threefold: (1) to develop a Brisbane River estuary and Moreton Bay flood model for various flows events under converging mesh size; (2) to conduct a simulation to assess the impact of compound riverine flooding and tides on water levels; and (3) to analyse the future storm surge effect on flood extent. The outcome of this study will be significant to comprehend the suitability of the hydrodynamic model to carry out flood modelling. Further, it will help to identify the flood-exposed areas and to apply possible remedial strategies to overcome the damage. The study results will help decision-makers to make a flood mitigation and management plan of action.

The paper is structured as follows: the case study area, Brisbane River estuary (BRE) is described in Section 2. Section 3 explains the Brisbane flooding, hydrodynamic model, the data requirements, and methods, including mesh resolution effect and compound flooding in BRE. The results of the hydrodynamic model calibration and validation along with mesh effects and compound flooding influence are described and discussed in Section 4. Finally, conclusions are specified in Section 5.

2 Study area

The Brisbane River and Moreton Bay are located on the southeast coast of Queensland, Australia (Fig. 1). The lower part of Brisbane River is termed the Brisbane River estuary (BRE). Moreton Bay is semi-closed coastal water situated at the mouth of Brisbane River. BRE and Moreton bay experience semidiurnal tides with a tidal range of 2.5 m. The Brisbane River has the longest course in sub-tropical SEQ, having a length of 344 km and has a catchment area of 13,600 km^2 (Eyre, Hossain, & McKee, 1998) to the Port Office Gauge which is located in the heart of Brisbane City.

https://doi.org/10.5194/nhess-2021-284
Preprint. Discussion started: 26 January 2022

The BRE is a micro-tidal estuary, with a mean spring and neap tidal range of 1.8 m and 1.0 m respectively (Wolanski, 2014). It has a tidal influence up to 80 km from the river mouth. The Oxley Creek and Bremer Rivers are major tributaries, which contribute to lower half catchment flows in BRE and join the estuary at 34 and 73 km respectively, from the river mouth. Estuary depth varies, from 15 m at the river mouth to about 4 m above Australian Height Datum (AHD) at the Bremer River junction at Moggill Point.

The catchment is manifold, joining rural and urban land, dams for flood mitigations, tidal impacts, and various tributaries with the prospect of flooding. The river system itself contains the Brisbane River and numerous main tributaries. The Brisbane River has two dams situated in its upper catchment, both of which were constructed with the twin objective of flood alleviation and water supply to Brisbane City. Wivenhoe dam regulates the flow of water in the upper part of Brisbane River, which is approximately 150 km upstream of the coast. The annual mean rainfall of the Brisbane River catchment is around 990 mm per year. In January 2011, a storm event caused widespread inundation on BRE floodplains (van den Honert & McAneney, 2011). Further, the 2013 storm and tidal influence caused mild inundation in BRE.

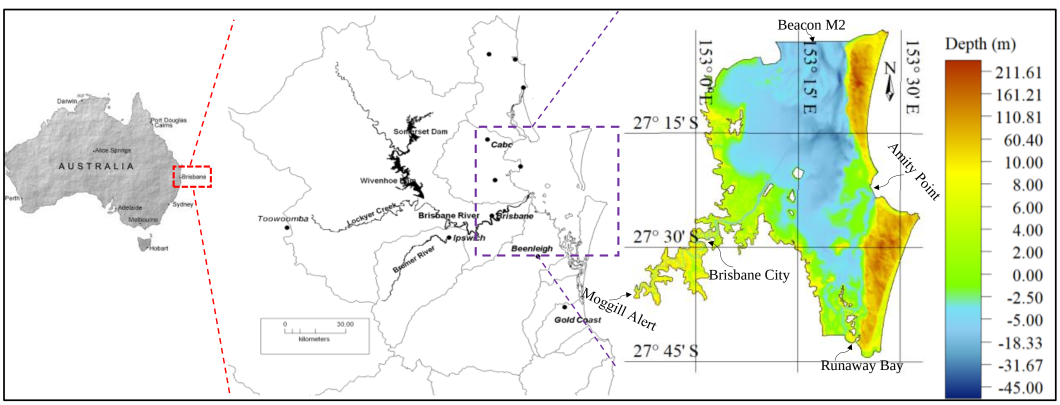

Fig 1: Brisbane River catchment and Moreton Bay

https://doi.org/10.5194/nhess-2021-284
Preprint. Discussion started: 26 January 2022

Natural Hazards and Earth System Sciences
Open Access
Discussions

3 Materials and methods

This study utilizes the MIKE 21 FM to explore the hydrodynamics and flood inundation in BRE. The MIKE-21 hydrodynamic model is built with various fine resolution mesh data and a time series of observed water levels and discharges were used to force model boundaries. Observed flood extent imagery, tidal gauges and water level were used for modelling results validation. By modelling the involved flooding drivers individually and jointly, we compute differences in flood risk estimation resulting from a separation of riverine and tide processes in coastal flood modelling. The modelling process, calibration and validation of the model followed in this study is presented in a flow chart as shown in Fig. 2.

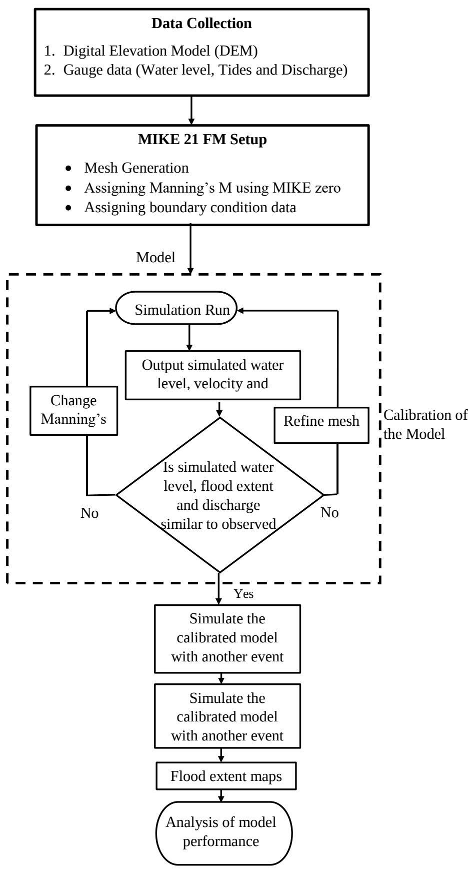

Fig. 2: Flowchart of processes involved in the MIKE 21 hydrodynamic simulation

https://doi.org/10.5194/nhess-2021-284
Preprint. Discussion started: 26 January 2022

Natural Hazards and Earth System Sciences
Discussions

3.1 Data collection

To carry out this study we have collected, DEM bathymetry data, water level, flow data, tidal data, flood measurement data, and flood extent satellite data. Data collected for the study with its resolution and sources are shown in Table 1.

Table 1. Data collected and sources for the study

Data	Description	Station No	Sources
DEM data	Brisbane River and floodplains; 5m x 5m DEM	N/A	Queensland Government under the Brisbane River Catchment Flood Study (BRCFS)
	Moreton Bay; 30m x 30m DEM	N/A	James Cook University (JCU) 3DGBR: GBR100 High-resolution
River gauge data (instantaneous values)	Moggill Alert	540200	Bureau of Meteorology, Queensland
	Jindalee	540192	
	Brisbane City Alert	540198	
Flow data (daily)	Savage crossing	143001	Water Monitoring Information Portal, Queensland Government
Tidal data (10 minutes interval)	Beacon M2 Moreton Bay	046206A	Maritime Safety Queensland
	Runaway Bay	045100B	
	Amity Point	046211E	
	Brisbane Bar	046046A	
	Whyte Island Alert	540495	
Flood extent (2011 and 2013)	Brisbane River flood extent	N/A	Queensland Government, Flood imagery and data

3.2 Hydrodynamic model

The model used in this study is DHI MIKE-21 FM, which is a two-dimensional (2D), depth-averaged hydrodynamic model, with a numerical solution based on the incompressible Reynolds averaged Navier-Stokes equations while using the finite volume method to solve the shallow water equations (DHI, 2017a). In the shallow water hydrodynamic equations, due to the stability constraint of the explicit scheme, the Courant-Friedrich-Levy (CFL) condition needs to be fulfilled, which can be calculated in Eq. 1. Critical CFL values are recommended to be set at 0.8, to fully secure the stability of the numerical scheme (DHI, 2014)

https://doi.org/10.5194/nhess-2021-284
Preprint. Discussion started: 26 January 2022

$$CFL_{HD} = \left(\sqrt{gh} + |u|\right)\frac{\Delta t}{\Delta x} + \left(\sqrt{gh} + |v|\right)\frac{\Delta t}{\Delta y} \tag{1}$$

Where h, is the local water depth; Δt is the interval of time step; Δx and Δy are typical length scales of meshes in the x and y direction respectively, u and v are the velocity components. The governing equation may not account for the wrong topography representation and its subsequent errors in the results. The correct discretization of mesh elements and limiting CFL can lead to correct results. MIKE 21 governing equations are attained by the integration of the horizontal momentum and continuity equation over depth h=$\eta + d$; the following shallow water 2-D equations are defined in Eqs (1-3):

$$\frac{\partial h}{\partial t} + \frac{\partial h\bar{u}}{\partial x} + \frac{\partial h\bar{v}}{\partial y} = hS \tag{2}$$

$$\frac{\partial h\bar{u}}{\partial t} + \frac{\partial h\bar{u}^2}{\partial x} + \frac{\partial h\bar{v}\bar{u}}{\partial y} = \mathrm{f}\bar{v}h - gh\frac{\partial \eta}{\partial x} - \frac{h}{\rho_o}\frac{\partial P_a}{\partial x} - \frac{gh^2}{2\rho_o}\frac{\partial \rho}{\partial x} + \frac{\tau_{sx}}{\rho_o} + \frac{\tau_{bx}}{\rho_o} - \frac{1}{\rho_o}\left(\frac{\partial s_{xx}}{\partial x} + \frac{\partial s_{xy}}{\partial y}\right) + \frac{\partial (hT_{xx})}{\partial x} + \frac{\partial (hT_{xy})}{\partial y} + hu_s \tag{3}$$

$$\frac{\partial h\bar{v}}{\partial t} + \frac{\partial h\bar{v}\bar{u}}{\partial x} + \frac{\partial hv^2}{\partial y} = \mathrm{f}\bar{u}h - gh\frac{\partial \eta}{\partial y} - \frac{h}{\rho_o}\frac{\partial P_a}{\partial y} - \frac{gh^2}{2\rho_o}\frac{\partial \rho}{\partial y} + \frac{\tau_{sy}}{\rho_o} + \frac{\tau_{by}}{\rho_o} - \frac{1}{\rho_o}\left(\frac{\partial s_{yx}}{\partial x} + \frac{\partial s_{yy}}{\partial y}\right) + \frac{\partial (hT_{xy})}{\partial x} + \frac{\partial (hT_{yy})}{\partial y} + hv_sS \tag{4}$$

Where t is the time, x and y are Cartesian coordinates, h is the water depth, s is the discharge, ρ_o is reference density of water, ρ is water density, P_a is atmospheric pressure (P_a), s_{xx} , s_{yx} , s_{yy} , s_{xy} are radiation stress components, $\bar{v}$, $\bar{u}$ are y and x directions depth-averaged velocity, τ_{xx} , τ_{xy} , τ_{yx},

https://doi.org/10.5194/nhess-2021-284
Preprint. Discussion started: 26 January 2022

τ_{yy} are lateral stress components, τ_{sx} , τ_{sy} are surface wind stress components, g is the acceleration due to gravity, f is Coriolis parameter, v_s, u_s are velocity by which water is discharged into the ambient water, τ_{bx}, τ_{by} are bottom stress components and η is water surface elevation.

The Flow Model of MIKE 21 is the basic hydrodynamic module. It provides the hydrodynamic basis for the computations of coastal hydraulics. It models the flows and variations of water level in response to a range of forcing functions on floodplains, lakes, estuaries, and coastal areas. Many researchers have successfully used the MIKE 21 FM model to investigate the hydrodynamic process of a large river and coastal bay, like Dongting Lake, China (Y. Liu et al., 2019) the Poyang Lake, China (Li & Yao, 2015; Li, Zhang, Tan, & Yao, 2020), Brisbane River estuary (Khalil et al., 2020), Vembanad Lake, India (Haldar, Khosa, & Gosain, 2019), Lake Alexandrina (J. Liu, Sivakumar, Yang, & Jones, 2018) and Deer Creek in the City of Brentwood (Shrestha et al., 2020). The MIKE 21 FM hydrodynamic module was used to simulate the depth-averaged flow features for the years 2006, 2011 and 2013 of the Brisbane River and Moreton Bay.

3.3 Mesh generation and cell size convergence

The DHI MIKE mesh generation tool allows the user to design the element resolution by describing the maximum element area, A_{max}. For the majority of mesh structure elements, approximate equilateral triangles can be attained in DHI MIKE (DHI, 2012) and the length of Δx is approximately calculated using Eq. 5, where $\theta \approx 60$;

$$\Delta x_{max} = 2\sqrt{A_{max}\,.\tan(\theta/2)} \tag{5}$$

In CFL_{HD} Eq. 1, as the local flow velocity is very less as compared to the local water depth so, it is reasonable to disregard the velocity terms, and the CFL_{HD} can be rewritten as Eq. 6 and further, the CFL_{HD} is rearranged to Eq. 7 with the reasonable assumption of $\Delta x \approx \Delta y$.

https://doi.org/10.5194/nhess-2021-284
Preprint. Discussion started: 26 January 2022

$$CFL_{HD} = \sqrt{gh}\frac{\Delta t}{\Delta x} + \sqrt{gh}\frac{\Delta t}{\Delta y} \tag{6}$$

$$CFL_{HD} = \sqrt{gh}\frac{\Delta t}{\sqrt{A_{max}}\,.\tan(\theta/2)} \leq 0.8 \tag{7}$$

Five meshes were generated and gradually attuned until all elements fulfilled the constraint in Eq. 7. Mesh quality was further enhanced by the smoothing tool to increase spatial regularity. The details of the elements, nodes, element areas CFL_{max} and simulation running time in each case are given in Table 2. For the case 1 mesh file, the A_{max} is 5 km^2 and A_{min} is 70 m^2, generating 95,497 elements covering the Brisbane River estuary with floodplain and the entire Moreton Bay. The mesh sizes were reduced in each subsequent case and in case 5 the mesh elements were 288,415. The five mesh cases with different element sizes for a small region near Brisbane city are shown in Fig. 3. In these five cases, element sizes were distributed with finer elements inside the Brisbane River and coarser elements inside Moreton Bay. In all cases, the time step, Δt, was set as 30 seconds to fulfil the critical CFL_{HD} of 0.8. A larger number of elements were estimated to involve a much lengthier time to complete the simulations. For the one month simulation of the flood event in BRE and Moreton Bay, the running time was approximately 11, 13, 18, 28 and 36 hours for each case, respectively.

Table. 2. Statistics of mesh convergence cases

	Case 1	Case 2	Case 3	Case 4	Case 5
Number of elements	95,497	122,220	153,383	217,066	288,415
Number of nodes	48,215	61,605	77,352	11,3116	148,697
Element area max. x10^4 (m^2)	500	100	30	15	10
Element area min. (m^2)	70	59.9	46.7	27.3	21.5
CFL_{max}	0.53	0.57	0.65	0.74	0.79
Running time (Hours)	11	13	18	28	36

Cell size convergence was performed until the increase or decree of cell size of the mesh make an effect on water levels. When the results were consistent, then we used the coarser-resolution with confidence, otherwise, we reduced the cell size until we got a consistent value.

https://doi.org/10.5194/nhess-2021-284
Preprint. Discussion started: 26 January 2022

Natural Hazards and Earth System Sciences
Open Access
Discussions

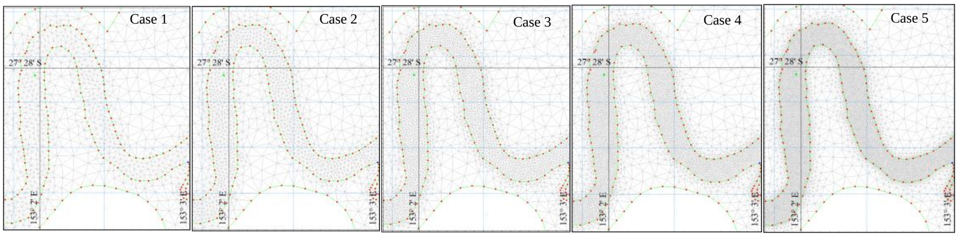

Fig. 3. Five cases of mesh convergence near the Brisbane city used in the modelling

The bathymetric data, longitudinal profile and cross-section comparison are shown in Fig. 4. It can be seen that by using coarser cell size and with uncontrolled data the cross-section representation changed as compared to finer cell and controlled data (Fig. 4e)

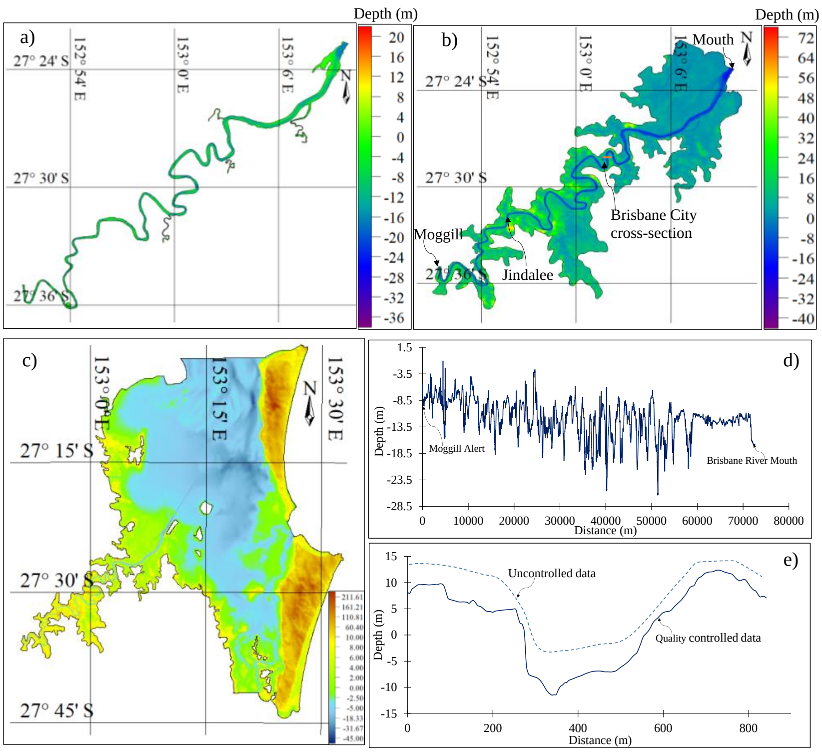

Fig. 4: Bathymetry of a) Brisbane River; b) Brisbane River and floodplain; c) Brisbane river floodplains and Moreton Bay; d) Longitudinal profile of Brisbane river; e) Brisbane river cross-section at Brisbane city

https://doi.org/10.5194/nhess-2021-284
Preprint. Discussion started: 26 January 2022

Natural Hazards and Earth System Sciences Open Access Discussions EGU

3.4 Future scenarios of storm surge

Tropical cyclones at some hundred kilometers north of Moreton Bay cause high waves and storm surge inside Moreton Bay. These events usually do not produce storm winds within Moreton Bay; however, can produce big ocean swell waves. It has been recognized that the wave circumstances produced from far away cyclones can cause a deviation of Moreton Bay water levels (Treloar, Taylor, & Prenzler, 2011). The mixture of storm surge and the normal tide is known as a storm tide and disastrous impacts occur when the storm surge coincides with an existing high tide. As a result, the storm tide can have an influence further upstream in the estuary. The ongoing sea-level rise will cause a rise in river tail-water levels, particularly in the storm surge. As the sea-level rise projections range is wide enough, while along the Australian coast, sea-level growth maybe 10% higher (IPCC, 2007). Ayre, Diermanse, L, and Hart (2017) provided the cases of flood simulation for four periods of future climate changes i.e. 2030, 2050, 2070 and 2100, in the BRE which is shown in Table 3. Based on these four scenarios, storm tide inputs at Brisbane bar (Fig. 5) were used to simulate the flooding behavior in BRE under low flow events.

Table 3: Proposed climate parameters for inclusion in BRE flood risk study

Scenario (S)	Years	Storm tide level
Base Scenario	Present	-1.5 to 1.5m
Scenario 1	2030	25% increase to the base case
Scenario 2	2050	50 % increase to the base case
Scenario 3	2070	75 % increase to the base case
Scenario 4	2100	100 % increase to the base case

https://doi.org/10.5194/nhess-2021-284
Preprint. Discussion started: 26 January 2022

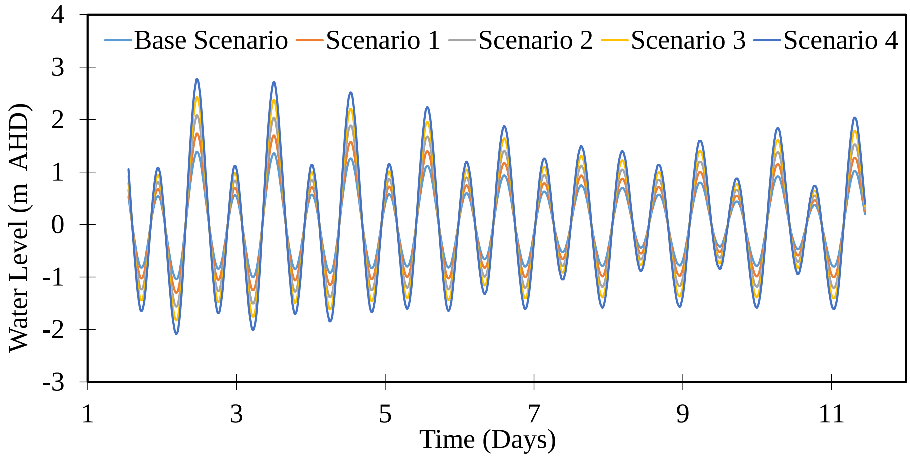

Fig 5: Input data for various scenarios of storm surge tide at Brisbane Bar

3.5 Model Setup

In the model, five meshes were generated the element sizes were adjusted by mesh convergence test and finally a range from 34 m^2 to 100,000 m^2, with a total of 288,415 unstructured elements and 148,697 nodes were used in the MIKE 21 domain area. The observed time-varying water level was used as the upstream boundary to the hydrodynamic model, and the tidal level observations at three stations (i.e., Amity Point, Runaway Bay Point, and at Beacon M2 Point) were adopted to set the lower boundary condition of the model (Fig). The model was initially set up by using bathymetric data of Brisbane River (Fig. 4a) and 2006 low flow data and tidal data as boundary conditions (Fig. 6 a&b). Then the model was extended to floodplain area (Fig. 4b) and the years 2013 and 2011 flood and tidal data (Fig. 6 c&d) were used for the model performance. Finally, the model included BRE and Moreton bay (Fig. 4c) with 2011 flood and tidal data (Fig. 6 e-h).

Currently, the MIKE-21 model has not considered evaporation, precipitation, wind direction, and wind speed. The initial water surface elevation of 0.1 m was used, while the initial water flow velocities were fixed to zero across the model area. The minimum time step is limited to 0.1 s to

https://doi.org/10.5194/nhess-2021-284
Preprint. Discussion started: 26 January 2022

Natural Hazards and Earth System Sciences
Discussions

keep the target Courant-Friedrichs-Lewy (CFL) number below 1.0. The thresholds h_{dry} (drying depth = 0.005 m) < h_{flood} (flooding depth = 0.05 m) < h_{wet} (wetting depth = 0.1 m) were used to describe the change of wetting and drying in the model (Li et al., 2020). In a hydrodynamic model, bed resistance is an important factor that controls river flow behaviour. While calibrating the model, Manning's n is changed within an acceptable limit to bridge the gap between observed and simulated water levels. Manning's M (reciprocal to Manning's n) is used in the model to specify the bed resistance. In the present study, the Manning number for the Brisbane River-floodplains and Moreton Bay is used as (M= 10–38 $m^{1/3}/s$) which was based on literature values from previous modelling calibration of Brisbane River (X. Liu & Lim, 2017; Yu, 2017) and Moreton Bay (Barton et al., 2017). The Smagorinsky factor of eddy viscosity (Cs = 0.28) based on the literature review (DHI, 2017b; Li et al., 2020) was adopted to perform the hydrodynamic simulation and model validation. Model calibration and validation are described in detail in section 4.

3.6 *Model performance evaluation indices*

To compare the observed and simulated results various statistic methods were used e.g. Nash-Sutcliffe model efficiency coefficient (E), Root Mean Square Error (RMSE) and Coefficient of determination (R^2). Nash-Sutcliffe coefficient (E) was used to assess MIKE 21 model predictive power and to describe quantitatively the accuracy of simulation results with the observed values. It is defined in Eq. 8:

$$E = 1 - \frac{\sum_{i=1}^{n} (X_{obs,i} - X_{model})^2}{\sum_{i=1}^{n} (X_{obs,i} - \overline{X_{obs}})^2} \tag{8}$$

Where X_{model} is simulated values at the time i and X_{obs} are observed values. Primarily, model efficiency close to 1, represent accurate results. Root mean square error (RMSE) was used to measure the difference between simulated values by a model and the observed values, it is defined in Eq. 9:

https://doi.org/10.5194/nhess-2021-284
Preprint. Discussion started: 26 January 2022

$$RMSE = \sqrt{\frac{\sum_{i=1}^{n}(X_{obs,i} - X_{model,i})^2}{n}} \tag{9}$$

Where, X_{model} is simulated values at the time i, X_{obs} is observed values

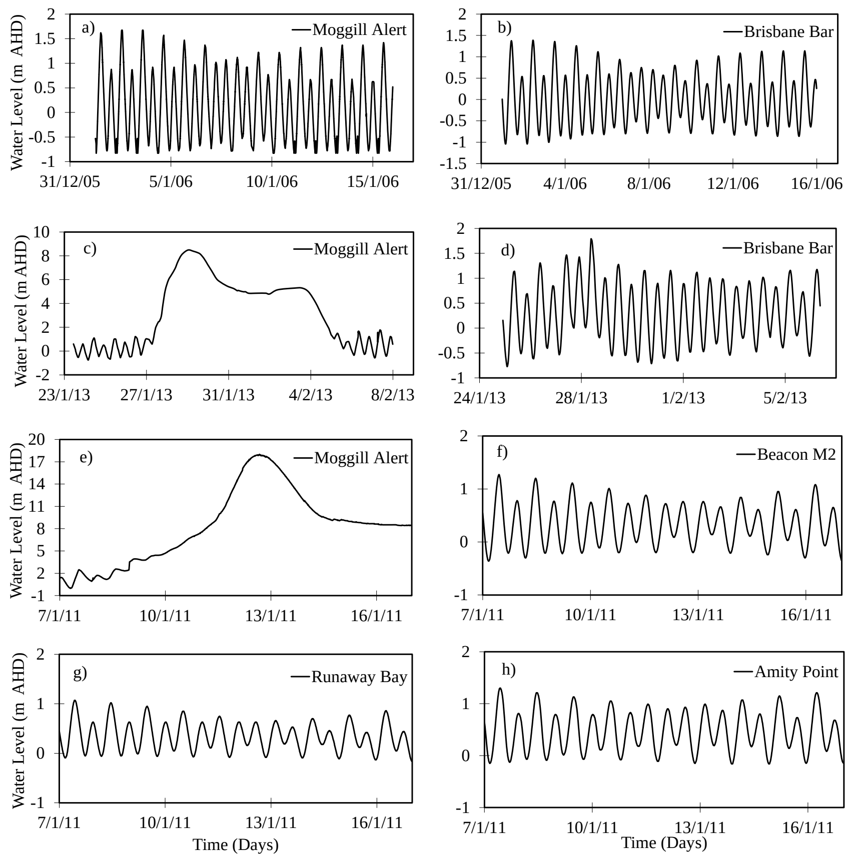

Fig. 6: MIKE 21 model input boundary water level and tidal data

4 Results and discussion

4.1 Calibration and validation of the model

A comparison between simulated and observed water levels at Brisbane City gauge for the low flow event confined inside the Brisbane River during the year 2006 is shown in Fig. 7a. For the year 2013 high flow event, spreading over floodplains, the comparison between observed and simulated water

https://doi.org/10.5194/nhess-2021-284
Preprint. Discussion started: 26 January 2022

level at Brisbane City gauge is shown in Fig. 7b. The hydrodynamic model is calibrated against the low flow event 2006, 2013 and to increase the predictive power it is validated for the high flow event of 2011. For the year 2011 flood event, extending over floodplains, the simulated results are compared with those observed at Brisbane City and Brisbane Bar gauge as shown in Fig. 7 (c&d). The performance indices for calibrating gauging stations are shown in Table 4. The statistical results showed that E_{ns} of water level's varied from 0.84 to 0.95, RMSE values are less than 0.3 and R^2 values varied from 0.85 to 0.96, which shows a good match between the observed and simulated water levels.

Table 4: Performance indices for the calibration and validation of gauging stations of the 2006, 2013 and 2011 flow events

Year	Gauging stations	RMSE	E_{ns}	R^2
2006	Brisbane City	0.25	0.84	0.85
2013		0.2	0.87	0.88
2011		0.3	0.94	0.95
	Brisbane Bar	0.1	0.95	0.96

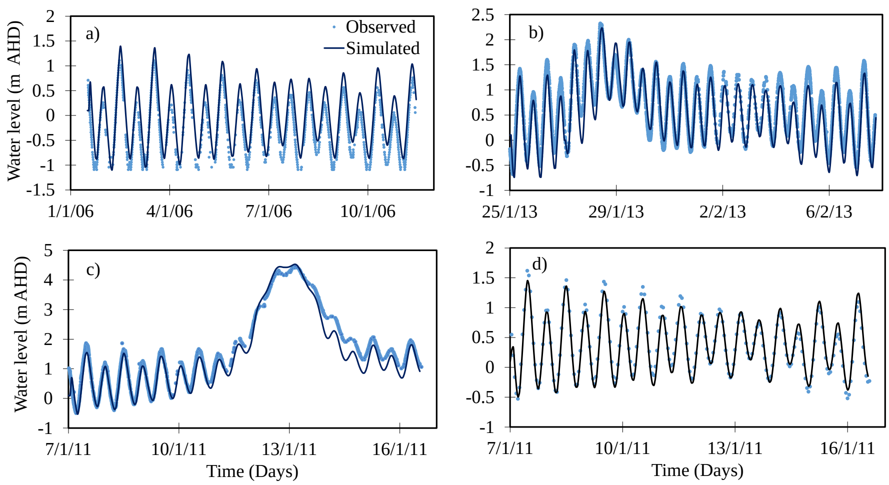

Fig. 7: Observed and simulated water levels at a) Brisbane City for the year 2006; b) Brisbane City for the year 2013; c) Brisbane city for the year 2011 and d) Brisbane Bar for the year 2011.

https://doi.org/10.5194/nhess-2021-284
Preprint. Discussion started: 26 January 2022

The result of the comparison between observed and simulated flood extent is shown in Fig. 8. Brisbane City experienced a major flood from 12th January 10:00 am to 13th January 6:00 pm of 32 hours duration (van den Honert & McAneney, 2011). The observed flood extent on 13th January 2011 at 04:00 am compared well with the simulated flood extent. The model predictions of flood extent are 90% accurate while using mesh case 5, which are substantially improved as compared to (X. Liu & Lim, 2017) with 66.9 % accuracy. The model correctly regenerated most of the Oxley Creek floodplain and the largest areas of observed flooding below the Jindalee floodplain (Fig. 8), due to the correct representation of bathymetry and boundary data which leads to correct flood extend assessment as discussed by (Shrestha et al., 2020). However, the model underestimated the flood extent in very small tributaries adjoining the Brisbane River, due to the lack of a very finer mesh size in these areas, because it would lead to an increase in computational time. Based on the model's good representation for the majority of the floodplain areas, the results can be used for future predictions.

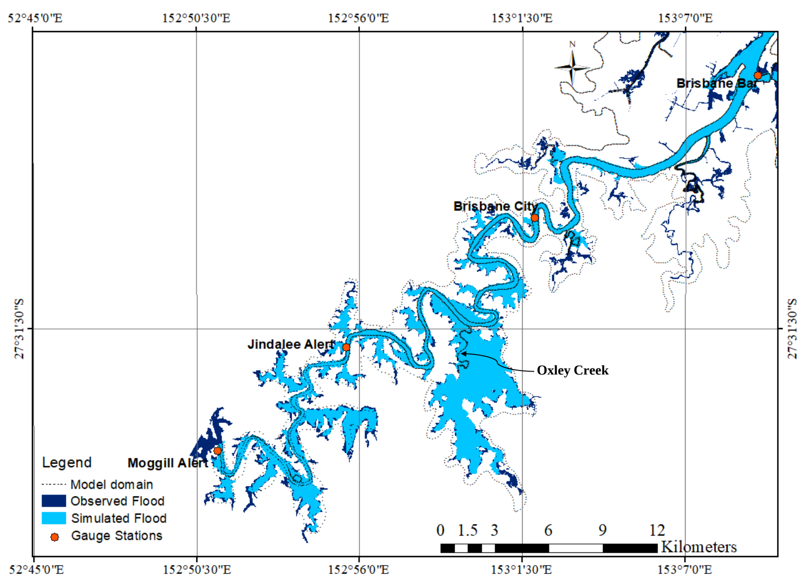

Fig. 8: Simulated and observed inundation area of Brisbane catchment for 2011 flood event

https://doi.org/10.5194/nhess-2021-284
Preprint. Discussion started: 26 January 2022

4.2 Mesh resolution effects on discharge

The model performance results for the simulated discharge by using different mesh resolutions at Brisbane City gauge is shown in Fig. 9. The results display a higher difference of coarser mesh with the observed data and as mesh size become finer the observed and simulated discharges reduce, indicating that the simulated discharges were correctly represented by the finer mesh resolution, as also proposed by (Teng et al., 2017). The percentage difference of peak value of simulated discharges with estimated discharge by Barton et al. (2017) was 16.54%, 14%, 12.19%, 2.88% and 2.7% from Case 1 to Case 5 respectively. The decreasing difference with observed values showed that the quality of simulation results was gradually enhanced by refining the mesh size; conversely, further decreases in mesh size create comparatively less difference from cases 4 to 5. Further, it was found that with coarser mesh size, the hydrodynamics features (i.e. current velocity and discharge) of the BRE might not be reproduced in the simulation, however with finer mesh size the performance of the model was enhanced which agreed with the findings of other studies (Shrestha et al., 2020).

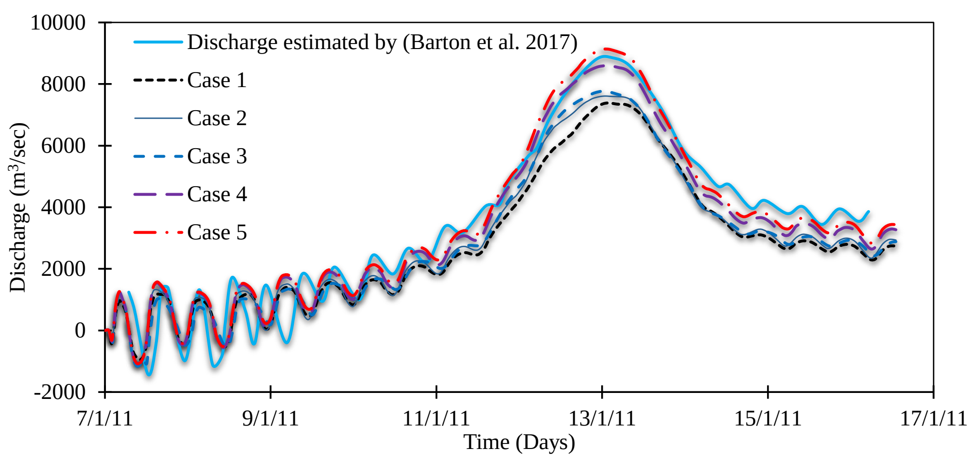

Fig. 9: Comparison of simulated discharge at Brisbane City gauge with estimated discharge by (Barton et al., 2017) for various mesh resolution cases

https://doi.org/10.5194/nhess-2021-284
Preprint. Discussion started: 26 January 2022

4.3 Modelled water levels and flood extents under varying boundaries

The results of the interaction of storm-tide and fluvial flooding mechanisms by modelling a compound flooding event in the BRE are shown in Fig. 10. The simulated and observed water levels with and without river and tidal boundaries are presented at three gauge locations in Fig. 10. The flood extents corresponding to these boundaries are presented in Fig. 11. Comparison of results at the Jindalee gauge station (Fig. 10a) with and without tidal boundaries show that the peak water level varied slightly, with a 0.62 m reduction at peak level without tidal input. Further, without tidal boundary, the hydrograph has attained smooth rising and falling limbs without showing any tidal variations. While, without discharge boundary i.e. Q=0, the tidal input moved up to the Jindalee gauge, and caused a slight reduction in tidal levels. The comparison of peak water level with and without tidal boundary at Brisbane City gauge (Fig. 10b) shows that the difference of peak flood level could be as high as 0.12 m, while without riverine boundary the water level followed the tidal wave pattern at Brisbane City gauge. At Brisbane bar, without tidal boundary, the water level followed a straight line, with a slight increase in water level during the flood days, while the tidal level at Brisbane Bar was slightly reduced without riverine boundary (Fig. 10c).

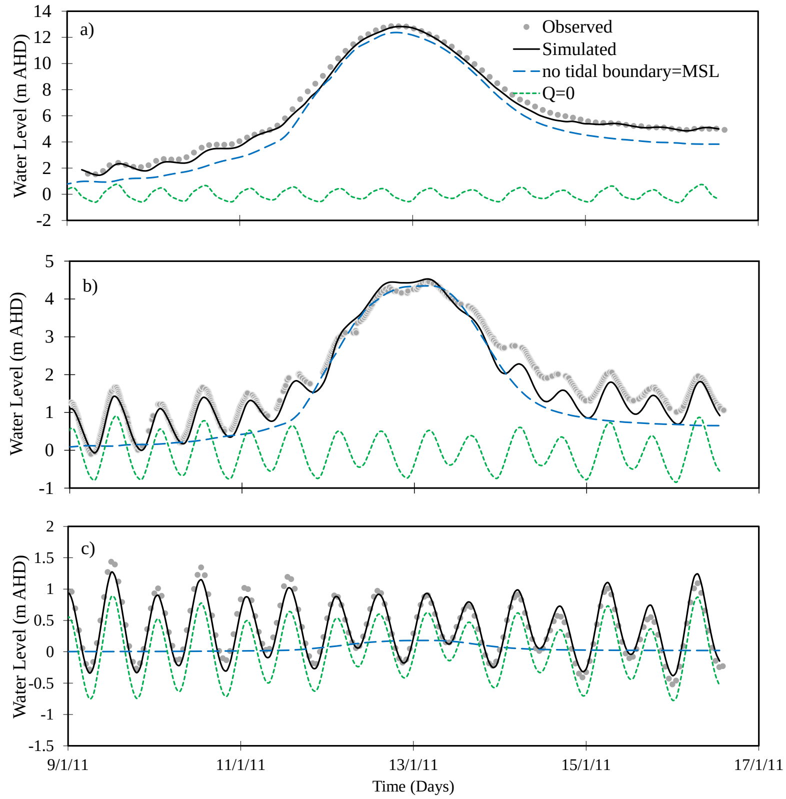

Fig. 10: Modelled and observed water levels for different boundaries (i.e. without tidal boundary = mean sea level (MSL); without discharge boundary, i.e., Q=0) at three gauges; a) Jindalee; b) Brisbane City and; c) Brisbane Bar

Modelled flood extents show a great difference between the two modelling set-ups. The spatial differences of flood extent resulting from simulations with and without river discharge are shown in Fig. 11. The flood extent resulting from the combination of river discharge and tidal water levels are shown as lighter blue areas in Fig. 11, whereas dark blue areas show the flood extent resulting only from tidal water inputs. The comparison of simulated flood extents resulting from these simulations shows variation in the lower BRE floodplain. The inclusion of river discharge caused substantial flood extent within the Oxley creek floodplain, while without river discharge the tidal

https://doi.org/10.5194/nhess-2021-284
Preprint. Discussion started: 26 January 2022

water level was confined within the BRE and caused flood extent in floodplain areas.

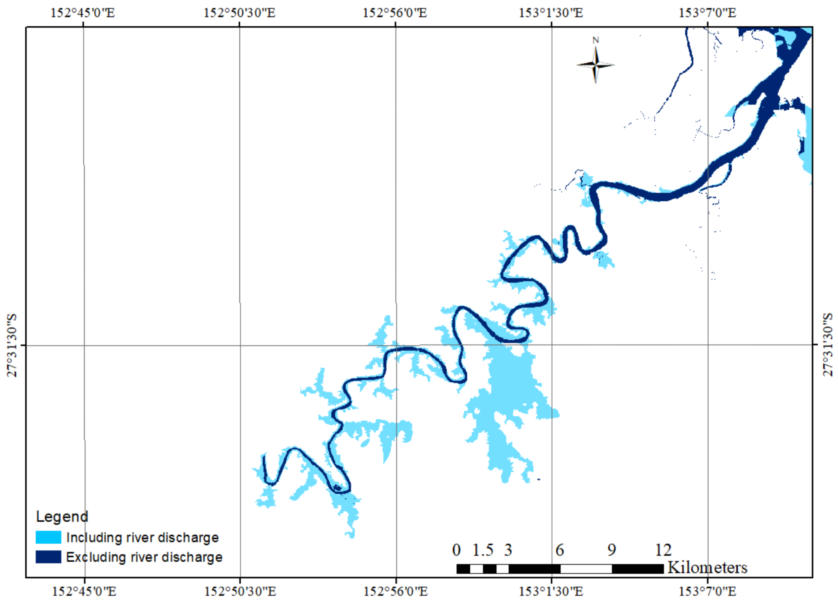

Fig. 11. Simulated maximum flood extents at Brisbane catchment for 2011 flood with and without river discharge using the two open boundary model setup.

4.4 Modelled flood extents under future storm surge cases

Simulated results of flood extent in BRE based on four storm surge scenarios (Fig. 4) are presented in Fig. 12. The normal tide flows inside the BRE, without causing any flooding. For future Scenario 1, with a 25% increase in tidal level, the tidal input mainly remained inside the BRE, while causing very minor flooding near the estuary mouth (Fig. 12 a). The tidal level inside the BRE was just below the minor flood level of 1.7 m. In Scenario 2, with a 50% increase in tidal level, the tidal level crossed the minor flood level and tidal inflow caused flooding in the tributaries adjoining the BRE (Fig. 12b). However, with Scenarios 3 and 4, the flood extent increased near the BRE mouth and Brisbane City gauge area (Fig. 12 c&d). Further, the flood water level surpassed the minor flood level and levelled with a medium flood level of 2.6 m in Scenario 3 and 4 respectively.

https://doi.org/10.5194/nhess-2021-284
Preprint. Discussion started: 26 January 2022

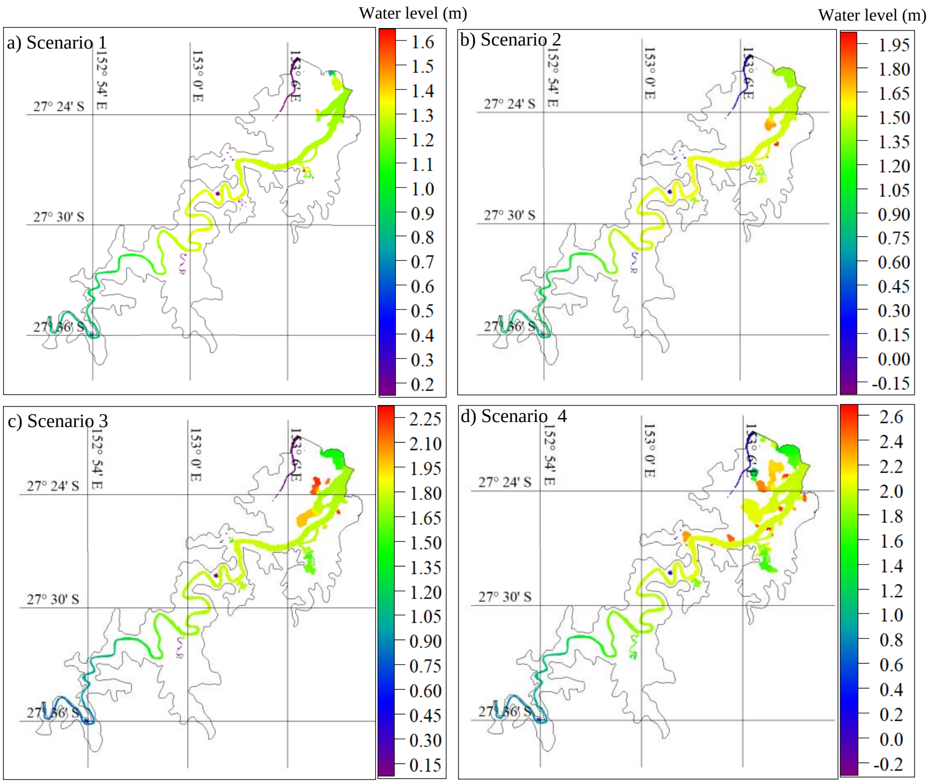

Fig. 12. Simulated flood extents of Brisbane catchment of four scenarios of storm surge

Further, the storm surge scenario 4 was analyzed, with the 2011 and 2013 floods in BRE and the flood extents are demonstrated in Fig. 13. The floodwater level during the 2011 flood at Brisbane city gauge was observed as 4.46 m, while considering the future storm surge scenario the flood water at Brisbane City gauge increased to 5 m due to the joint probability of riverine and tidal effects and hence flooding extent and depth increase in the floodplain area, with more flooding at the BRE mouth (Fig. 13 a). Similarly, the flood height for the 2013 flood increased from 2.24 m to 3.01 m due to the joint probability of river and storm surge, crossing the medium flood level of 2.6 m at Brisbane city gauge and leading to flooding in the Oxley creek area (Fig. 13 b). The modelling with the future storm surge scenarios has shown that for flood inundation study and coastal planning in BRE, the combination of riverine flow and the storm surge effect due to climate change were considered. As

https://doi.org/10.5194/nhess-2021-284
Preprint. Discussion started: 26 January 2022

with the increasing tidal height, the tidal impact pushed low river flow, while moving along the BRE beyond Moggill gauge, and causing minor and moderate flooding.

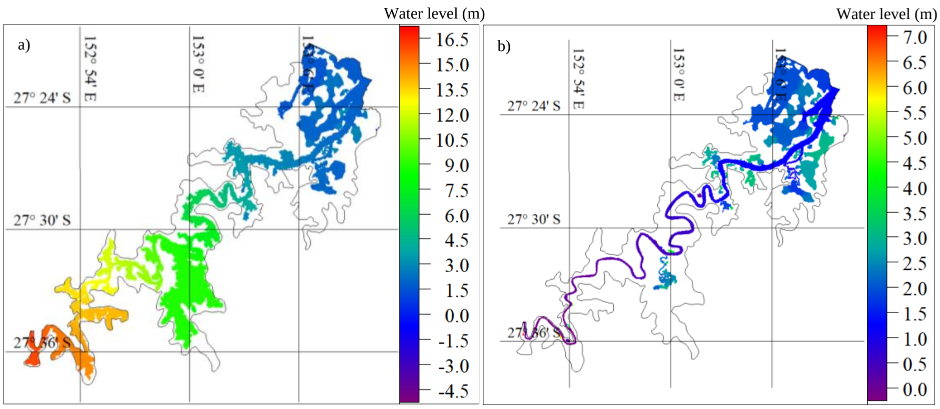

Fig. 13. Simulated flood extents of Brisbane catchment; a) 2011 and; b) 2013 flood events in combination with future storm surge scenario 4

5 Conclusions

To simulate flood height and extent in Brisbane River Estuary, mesh resolutions and combined flood effect by using the MIKE 21 Model were analysed. MIKE 21 hydrodynamic model was calibrated and validated for the years 2006, 2013 and 2011 flow events, with a flow Nash–Sutcliffe coefficient (E) between 0.84 and 0.95 at all gauges. The model simulated the flooding extent of BRE showing more than 90% accuracy. This confirmed that the MIKE 21 model can dynamically simulate and replicate the flows with a compound flood event.

Five mesh resolutions cases were analyzed and the result found that finer mesh resolution produces more accurate results and performs better with hydrodynamic features. Moreover, model performance evaluation showed that the mesh structure in Case 5 was more appropriate than the others, considering the convergence tendency of the simulation results and running time.

https://doi.org/10.5194/nhess-2021-284
Preprint. Discussion started: 26 January 2022

Compound flood event simulation results emphasized that not considering the interaction of various flooding drivers have caused 0.62 m and 0.12 m reduction in flood levels at Jindalee and Brisbane City gauges while leading to substantial underestimation of flood extent. Results endorse the consideration of tidal and riverine flooding drivers mutually for coastal flood extents assessments in estuaries.

Simulated results of flood extent in BRE based on four storm surge scenarios show that the flooding level would cross the medium flood level at Brisbane City gauge. Further with 2011 and 2013 floods with storm surge scenario 4, it was demonstrated, that the flood level will increase to 12% and 34% respectively and flood extent will increase in Oxley creek and near the BRE mouth.

The results show that a flood hydrodynamics study of BRE using compound flood events and considering future storm surge analysis would be helpful for coastal managers for planning and management of coastal projects.

Author's contribution

U.K.: Conceptualization, methodology, writing—original draft, review editing and investigation. S.Y.: Conceptualization, review, editing, and supervision. M.S (Muttucumaru Sivakumar). Review editing and supervision. K.E.: Review, editing and supervision. M.S (Mariam Sajid): Investigation, writing, review and editing. M.Z.B.R.: Review and editing. All authors have read and agreed to the published version of the manuscript.

Declaration of Competing Interest

The authors declare that they have no known competing financial interests or personal relationships that could have appeared to influence the work reported in this paper.

Funding: This research received no external funding

Acknowledgments: The authors would like to thank the Queensland Government Departments for providing all necessary input data. Special thanks are to Daryl Metters (Department of Environment and Science), Jim Fear (SEQ Water), Paul Boswood (Department of Environment and Science), Paul Birch (Bureau of Meteorology) and Paul Finger (Maritime Safety Queensland).

https://doi.org/10.5194/nhess-2021-284
Preprint. Discussion started: 26 January 2022

We are thankful to DHI for providing the MIKE 21 license. The authors would also like to thank Caroline Lai and Méven Robin Huiban for providing the technical support for MIKE 21.

Conflicts of Interest: The authors declare no conflict of interest.

6 References

Apel, H., Thieken, A. H., Merz, B., Blöschl, G. J. N. H., & Sciences, E. S. (2004). Flood risk assessment and associated uncertainty. *4*(2), 295-308.

Ayre, R., Diermanse, F., L, T., & Hart, P. (2017). *Brisbane River Catchment Flood Study: Comprehensive Hydrologic Assessment, Aurecon Australasia, Brisbane, Queensland, Australia* Retrieved from

Barton, C., Syme, B., Ryan, J., Rodgers, B., & Jensen, R. (2017). *Milestone Report 2: Fast Model Development and Calibration Comprehensive Hydraulic Assessment, BMT WBM, Brisbane, Queensland, Australia*. Retrieved from

Barton, C., Wallace, S., Syme, B., Wong, W. T., & Onta, P. (2015). *Brisbane River catchment flood study: comprehensive hydraulic assessment overview.* Paper presented at the Floodplain Management Association National Conference, Brisbane, Australia.

Chen, A. S., Evans, B., Djordjević, S., & Savić, D. A. (2012). Multi-layered coarse grid modelling in 2D urban flood simulations. *Journal of Hydrology, 470-471*, 1-11. doi:10.1016/j.jhydrol.2012.06.022

Copernicus. (2021). Floodlist. Retrieved from https://floodlist.com/asia/world-floods-july-2021

DHI. (2012). MIKE ZERO, Mesh Generator, Step-by-step training guide.

DHI. (2014). MIKE 21 Hydrodynamic Module Step-by-step training guide.

DHI. (2017a). MIKE 21 & MIKE 3 Flow Model FM, Hydrodynamic and Transport Module Scientific Documentation.

DHI. (2017b). MIKE 21 Flow Model FM, Hydrodynamic Module, User Guide.

Eyre, B., Hossain, S., & McKee, L. (1998). A suspended sediment budget for the modified subtropical Brisbane River estuary, Australia. *Estuarine, Coastal and Shelf Science, 47*(4), 513-522.

Geravand, F., Hosseini, S. M., & Ataie-Ashtiani, B. (2020). Influence of river cross-section data resolution on flood inundation modeling: Case study of Kashkan river basin in western Iran. *Journal of Hydrology, 584*. doi:10.1016/j.jhydrol.2020.124743

Haldar, R., Khosa, R., & Gosain, A. (2019). Impact of Anthropogenic Interventions on the Vembanad Lake System. In *Water Resources and Environmental Engineering I* (pp. 9-29): Springer.

Hallegatte, S., Green, C., Nicholls, R. J., & Corfee-Morlot, J. (2013). Future flood losses in major coastal cities. *Nature climate change, 3*(9), 802.

Hawkes, P., & Svensson, C. (2006). Joint Probability: Dependence mapping and best practice. *T02-06-16*.

IPCC. (2007). Fourth Assessment Report of the IPCC.

IPCC. (2021). *Sixth Assessment Report, AR6 Climate Change 2021: The Physical Science Basis*. Retrieved from

Karim, M. F., & Mimura, N. (2008). Impacts of climate change and sea-level rise on cyclonic storm surge floods in Bangladesh. *Global Environmental Change, 18*(3), 490-500.

Khalil, U., & Khan, N. M. (2017). Floodplain Mapping for Indus River: Chashma–Taunsa Reach. *Pakistan Journal of Engineering and Applied Sciences*.

https://doi.org/10.5194/nhess-2021-284
Preprint. Discussion started: 26 January 2022

Natural Hazards and Earth System Sciences
Discussions

Khalil, U., Yang, S.-Q., Sivakumar, M., Enever, K., Sajid, M., & Bin Riaz, M. Z. (2020). Investigating an Innovative Sea-Based Strategy to Mitigate Coastal City Flood Disasters and Its Feasibility Study for Brisbane, Australia. *Water, 12*(10). doi:10.3390/w12102744

Kumbier, K., Cabral Carvalho, R., Vafeidis, A. T., & Woodroffe, C. D. (2018). Investigating compound flooding in an estuary using hydrodynamic modelling: a case study from the Shoalhaven River, Australia.

Lee, E. H., & Kim, J. H. (2018). Development of a flood-damage-based flood forecasting technique. *Journal of Hydrology, 563*, 181-194.

Leonard, M., Westra, S., Phatak, A., Lambert, M., van den Hurk, B., McInnes, K., . . . Stafford-Smith, M. (2014). A compound event framework for understanding extreme impacts. *Wiley Interdisciplinary Reviews: Climate Change, 5*(1), 113-128. doi:10.1002/wcc.252

Li, Y., & Yao, J. (2015). Estimation of transport trajectory and residence time in large river–lake systems: application to Poyang Lake (China) using a combined model approach. *Water, 7*(10), 5203-5223.

Li, Y., Zhang, Q., Tan, Z., & Yao, J. (2020). On the hydrodynamic behavior of floodplain vegetation in a flood-pulse-influenced river-lake system (Poyang Lake, China). *Journal of Hydrology, 585*. doi:10.1016/j.jhydrol.2020.124852

Liu, J., Sivakumar, M., Yang, S., & Jones, B. G. (2018). *Salinity Modelling and Management of the Lower Lakes of the Murray–Darling Basin, Australia*. Paper presented at the Water Pollution XIV.

Liu, X., & Lim, S. (2017). Flood Inundation Modelling for Mid-Lower Brisbane Estuary. *River Research and Applications, 33*(3), 415-426.

Liu, Y., Yang, S.-Q., Jiang, C., Sivakumar, M., Enever, K., Long, Y., . . . Yin, L. (2019). Flood Mitigation Using an Innovative Flood Control Scheme in a Large Lake: Dongting Lake, China. *Applied Sciences, 9*(12), 2465.

Mani, P., Chatterjee, C., & Kumar, R. J. N. H. (2014). Flood hazard mapping and flood risk assessment using remote sensing, GIS and hydraulic modeling techniques. *70*, 1553-1574.

McCallum, I., Liu, W., See, L., Mechler, R., Keating, A., Hochrainer-Stigler, S., . . . Arestegui, M. (2016). Technologies to support community flood disaster risk reduction. *International Journal of Disaster Risk Science, 7*(2), 198-204.

Neumann, J. E., Price, J., Chinowsky, P., Wright, L., Ludwig, L., Streeter, R., . . . Martinich, J. (2014). Climate change risks to US infrastructure: impacts on roads, bridges, coastal development, and urban drainage. *Climatic change, 131*(1), 97-109. doi:10.1007/s10584-013-1037-4

O'Connor, J. E., & Costa, J. E. (2004). *The world's largest floods, past and present: their causes and magnitudes*: Geological Survey (USGS).

Pachauri, R. K., Allen, M. R., Barros, V. R., Broome, J., Cramer, W., Christ, R., . . . Dasgupta, P. (2014). *Climate change 2014: synthesis report. Contribution of Working Groups I, II and III to the fifth assessment report of the Intergovernmental Panel on Climate Change*: Ipcc.

Pellikka, H., Leijala, U., Johansson, M. M., Leinonen, K., & Kahma, K. K. (2018). Future probabilities of coastal floods in Finland. *Continental shelf research, 157*, 32-42. doi:10.1016/j.csr.2018.02.006

Queensland Floods Commission Inquiry Report, Q. (2011). *Queensland Floods Commission of Inquiry, Complete list of Final Report recommendations*. Retrieved from

Sadler, J. M., Goodall, J. L., Behl, M., Bowes, B. D., & Morsy, M. M. (2020). Exploring real-time control of stormwater systems for mitigating flood risk due to sea level rise. *Journal of Hydrology, 583*. doi:10.1016/j.jhydrol.2020.124571

Shrestha, A., Bhattacharjee, L., Baral, S., Thakur, B., Joshi, N., Kalra, A., & Gupta, R. (2020). *Understanding Suitability of MIKE 21 and HEC-RAS for 2D Floodplain Modeling*.

Smith, L. C. J. H. p. (1997). Satellite remote sensing of river inundation area, stage, and discharge: A review. *11*(10), 1427-1439.

Son, A.-L., Kim, B., & Han, K.-Y. (2016). A Simple and Robust Method for Simultaneous Consideration of Overland and Underground Space in Urban Flood Modeling. *Water, 8*(11). doi:10.3390/w8110494

Sulis, A., Frongia, S., Liberatore, S., Zucca, R., & Sechi, G. (2018). Combining water supply and flood control purposes in the Coghinas Basin (Sardinia, Italy). *International Journal of River Basin Management*(just-accepted), 1-32.

Svensson, C., & Jones, D. A. (2004). Dependence between sea surge, river flow and precipitation in south and west Britain. *Hydrology and Earth System Sciences, 8*(5), 973-992.

Syme, B., Wallace, S., Rodgers, B., Jensen, R., & Barton, C. (2019). *Executive Summary and Recommendations Brisbane River Strategic Floodplain Management Plan, BMT WBM, Brisbane, Queensland, Australia*. Retrieved from

Teng, J., Jakeman, A. J., Vaze, J., Croke, B. F. W., Dutta, D., & Kim, S. (2017). Flood inundation modelling: A review of methods, recent advances and uncertainty analysis. *Environmental Modelling & Software, 90*, 201-216. doi:10.1016/j.envsoft.2017.01.006

Torres, J. M., Bass, B., Irza, N., Fang, Z., Proft, J., Dawson, C., . . . Bedient, P. (2015). Characterizing the hydraulic interactions of hurricane storm surge and rainfall–runoff for the Houston–Galveston region. *Coastal Engineering, 106*, 7-19. doi:10.1016/j.coastaleng.2015.09.004

Treloar, P., Taylor, D., & Prenzler, P. (2011). Investigation of wave induced storm surge within a large coastal embayment-Moreton Bay (Australia). *Coastal Engineering Proceedings*, *1*(32), 22.

Tsoukala, V. K., Chondros, M., Kapelonis, Z. G., Martzikos, N., Lykou, A., Belibassakis, K., & Makropoulos, C. (2016). An integrated wave modelling framework for extreme and rare events for climate change in coastal areas–the case of Rethymno, Crete. *Oceanologia, 58*(2), 71-89.

UNISDR, U. N. I. S. f. D. R. (2015). *Global Assessment Report on Disaster Risk Reduction 2015: Making Development Sustainable: the Future of Disaster Risk Management*: United Nations International Strategy for Disaster Reduction.

Van Coppenolle, R., & Temmerman, S. (2019). A global exploration of tidal wetland creation for nature-based flood risk mitigation in coastal cities. *Estuarine, Coastal and Shelf Science, 226*. doi:10.1016/j.ecss.2019.106262

van den Honert, R. C., & McAneney, J. (2011). The 2011 Brisbane floods: causes, impacts and implications. *Water, 3*(4), 1149-1173.

Vitousek, S., Barnard, P. L., Fletcher, C. H., Frazer, N., Erikson, L., & Storlazzi, C. D. (2017). Doubling of coastal flooding frequency within decades due to sea-level rise. *Sci Rep, 7*(1), 1399. doi:10.1038/s41598-017-01362-7

Wolanski, E. (2014). *Estuaries of Australia in 2050 and Beyond*: Springer.

Wu, W., Westra, S., & Leonard, M. (2020). Estimating the Probability of Compound Floods in Estuarine Regions. doi:10.5194/hess-2020-456

Yu, Y. (2017). Numerical Study of Hydrodynamic and Sediment Transport Within the Brisbane River Estuary and Moreton Bay, Australia.

Zheng, F., Westra, S., Leonard, M., & Sisson, S. A. (2014). Modeling dependence between extreme rainfall and storm surge to estimate coastal flooding risk. *Water Resources Research, 50*(3), 2050-2071. doi:10.1002/2013wr014616

https://doi.org/10.5194/nhess-2021-284
Preprint. Discussion started: 26 January 2022

Zheng, F., Westra, S., & Sisson, S. A. (2013). Quantifying the dependence between extreme rainfall and storm surge in the coastal zone. *Journal of Hydrology*, *505*, 172-187.